

NASA Technical Memorandum 84542

IMPROVEMENTS TO THE LANGLEY HZE ABRASION MODEL



Lawrence W. Townsend and Hari B. Bidasaria

September 1982



**(NASA-TM-84542) IMPROVEMENTS TO THE LANGLEY
HZE ABRASION MODEL (NASA) 21 p
HC A02/MF A01**

CSCL 20H

#83-13971

**Unclas
G3/73 02045**



**National Aeronautics and
Space Administration**

**Langley Research Center
Hampton, Virginia 23665**

Table of Contents

NOMENCLATURE.....	i
SUMMARY.....	1
INTRODUCTION.....	2
ANALYSIS.....	3
RESULTS.....	5
CONCLUDING REMARKS.....	7
REFERENCES.....	8
TABLES.....	10
FIGURES.....	11

Nomenclature

A	nuclear mass number
a	oscillator parameter, fm
$B(e)$	average slope parameter of nucleon-nucleon scattering amplitude, fm ²
\vec{b}	projectile impact parameter vector, fm
C	average correlation function
e	two-nucleon kinetic energy in their center of mass frame, GeV
k_F	Fermi momentum wavenumber, fm ⁻¹
$I(\vec{b})$	defined in equation (3)
n	number of abraded nucleons
N	neutron number
\vec{r}	position vector, fm
r_c	nucleon effective root-mean-square radius, fm

r_n	neutron root-mean-square charge radius, fm
r_p	proton root-mean-square charge radius, fm
\vec{y}	two-nucleon relative position vector, fm
Z	total number of nuclear protons
\vec{z}	position vector of projectile in beam direction, fm
$\binom{A}{n}$	binomial coefficient
ξ_T	collection of constituent relative coordinates for target, fm
ρ	nuclear density, fm ⁻³
$\sigma(e)$	average nucleon-nucleon total cross section, fm ² or mb
σ_{abs}	heavy-ion absorption cross section, fm ² or mb
σ_n	cross section for abrading n nucleons, fm ² or mb

Subscripts:

c **charge**

F **prefragment**

m **matter**

P **projectile**

p **proton**

T **target**

Arrows over symbols indicate vectors.

Improvements to the Langley HZE Abrasion Model

by

Lawrence W. Townsend, Langley Research Center, Hampton, Virginia

and

Hari B. Bidasaria, Old Dominion University, Norfolk, Virginia

Summary

Improvements to a previously developed HZE abrasion model are made by incorporating more realistic values for the constituent Fermi momentum and nucleon root-mean-square charge radius. The theoretical predictions for neon projectiles at 2.1 GeV/nucleon colliding with carbon and molybdenum targets are in excellent agreement with recent experiment results.

INTRODUCTION

The attractiveness of HZE attenuation by nuclear fragmentation, as a means of radiation protection for future manned space applications, dictates that a quantitatively accurate nuclear fragmentation model be developed. In previous work (refs. 1 and 2) an HZE abrasion model, which incorporates Pauli correlation effects and realistic density distributions, has been developed. In reference 2, the importance of Pauli effects and the proper choice for the nuclear density distribution were clearly demonstrated by comparison with recent experimental results (ref. 3). For simplicity, the constituent Fermi momentum chosen for use in that work was the value for infinite nuclear matter. In addition, the nuclear distributions were obtained by unfolding the finite proton charge distribution from the experimental nuclear charge densities. In this work, improvements in these two areas are made by utilizing more realistic values for the Fermi momentum (refs. 4 and 5) and by utilizing an "effective" nucleon charge distribution which accounts for the differences between the neutron and proton charge distributions (ref. 6).

ANALYSIS

From reference 2, the cross section for abrading projectile nucleons is

$$\sigma_n = \binom{A_p}{n} 2\pi \int \{1 - \exp[-A_T \sigma(e) I(\vec{b})]\}^n \exp[-A_T A_F \sigma(e) I(\vec{b})] b db \quad (1)$$

where the residual fragment (prefragment) mass number is

$$A_F = A_p - n \quad (2)$$

and $I(\vec{b})$ is

$$I(\vec{b}) = [2\pi B(e)]^{-3/2} \int d\vec{z} \int d^3\xi_T \rho_T(\xi_T) \int d^3\vec{y} \rho_p(\vec{b} + \vec{z} + \vec{y} + \xi_T) [1 - C(\vec{y})] \exp \frac{-y^2}{2B(e)} \quad (3)$$

The Pauli correlation function approximation $C(\vec{y})$, is

$$C(\vec{y}) = \frac{1}{4} \exp(-k_F^2 y^2 / 10) \quad (4)$$

where $k_F = 1.36 \text{ fm}^{-1}$ for infinite nuclear matter. Since infinite nuclear matter is approached only for very heavy nuclei (ref. 3), the corresponding Fermi momentum, although a reasonable approximation, is generally an overestimate, especially for

lighter nuclei. This can be seen from Table I which lists values for Fermi momenta (k_F) as a function of mass number, obtained from 500 MeV electron scattering experiments (ref. 4). The value for k_F is even smaller if the incident lab momentum per nucleon (drift momentum) is accounted for (ref. 5).

The nuclear densities, ρ_T and ρ_p , shown in equation (3) are obtained by unfolding the gaussian nucleon charge density from the experimental nuclear charge distribution using the methods of references 2 and 7. In those works, the nucleon charge density was assumed to be identical to that of a bare proton. Since the charge distribution of a proton differs from that of a neutron, we replace the bare proton rms radius by an effective nucleon rms charge radius (ref. 6) which accounts for this difference. From reference 6, it is

$$r_c^2 = r_p^2 - (N/Z) r_n^2 \quad (5)$$

where the bare proton rms radius is $r_p = 0.87$ fm (ref. 2) and the neutron rms radius is $r_n = 0.3359$ fm (ref. 8). In equation (5), N is the neutron number and Z the proton number for the nucleus under consideration.

RESULTS

Abrasion cross sections for neon-carbon collisions, using equation (1), are listed in Table II as a function of nucleon charge radius, r_C , and Fermi momentum, k_F . The values of r_C correspond to the bare proton (0.87 fm) and the effective nucleon radius (0.806 fm) obtained from equation (5). The values for k_F correspond to the infinite matter value (1.36 fm^{-1}), the value for the composite system ($A = A_p + A_T$ where $k_F = 1.23 \text{ fm}^{-1}$), and a representative value, from reference 5, which includes drift momentum effects (0.7 fm^{-1}). In order to compare these results with the experimental data of Stevenson et al (ref. 3), it is necessary to convert the abrasion cross sections into relative probabilities for the formation of a particular residual projectile fragment mass, A_F . The results of this procedure, which is described in detail in reference 2, are listed in Table III and displayed in figures 1 and 2. Also displayed in the figures are the experimental data of reference 3.

In figure 1 are displayed the results obtained for Ne+C in reference 2 ($r_C = 0.87 \text{ fm}$, $k_F = 1.36 \text{ fm}^{-1}$) and this work ($r_C = 0.806 \text{ fm}$, $k_F = 0.7 \text{ fm}^{-1}$) compared with the experimental data (ref. 3). The agreement between experiment and the results of this work is excellent. From Table III, analysis of the relative probabilities indicates that there is essentially no dependence of the relative probability on k_F . Note that Table II shows σ_{abs} decreasing as k_F decreases. All values of σ_{abs} listed in Table II, however, are in excellent agreement with the

experimental value of 1040 ± 60 mb (ref. 9). From figure 2 we see that the improved agreement with the experiment is due to incorporating the neutron charge distribution differences (from eq. (5)) into the effective nucleon charge distribution. The Fermi momentum was $k_F = 0.7 \text{ fm}^{-1}$ for both curves.

Figure 3 displays results obtained for Ne + Mo with $r_C = .80 \text{ fm}$ and $k_F = 0.7 \text{ fm}^{-1}$. In general, the agreement is quite good except when $A_F \leq 4$ where the theory overestimates the relative probabilities. The theoretical curve was determined using ^{96}Mo as a target. The experiment data were obtained for natural molybdenum which has 7 stable isotopes ($A = 92, 94, 95, 96, 97, 98, 100$) of roughly comparable abundance (9.04 percent to 23.78 percent). Unfortunately, experimental charge distribution data (ref. 8) are not available for all stable molybdenum isotopes so that a more exact theoretical analysis is not possible.

CONCLUDING REMARKS

By utilizing an effective nucleon charge distribution, rather than the bare proton distribution, to account for differences in the charge distributions within the proton and neutron, improved agreement between the predicted abrasion cross sections and recent experimental data were obtained. These findings also confirm the sensitivity of the abrasion results to the assumed nuclear distribution found in reference 2. In reference 2, the need for Pauli effects to be included were also clearly demonstrated. In this work, however, we find that once Pauli effects are included, the abrasion results are relatively insensitive (at 2.1 GeV/nucleon) to the actual value of Fermi momentum used, as long as it is physically realistic (less than the infinite matter value). Further confirmation of these findings and additional improvements to the theory will require additional experimental data.

REFERENCES

1. Townsend, L. W.: Optical-Model Abrasion Cross Sections for High-Energy Heavy Ions. NASA TP 1893, 1981.
2. Townsend, L. W.: Harmonic Well Matter Densities and Pauli Correlation Effects in Heavy-Ion Collisions. NASA TP 2003, 1982.
3. Stevenson, J. D.; Martinis, J.; and Price, P. B.: Measurement of the Summed Residual Projectile Mass in Relativistic Heavy-Ion Collisions. Physics Review Letters, vol. 47, no. 14, 1981, pp. 990-993.
4. Moniz, E. J.; Sick, I.; Whitney, R. R.; Ficenec, J. R.; Kephart, R. D.; and Trower, W. P.: Nuclear Fermi Momenta from Quasielastic Electron Scattering. Physics Review Letters, vol. 46, no. 8, 1971, pp. 445-448.
5. Vary, J. P.; and Dover, C. B.: Microscopic Models for Heavy Ion Scattering at Low, Intermediate and High Energies. Proceedings of the Second High Energy Heavy Ion Summer Study, LBL-3675, Lawrence Berkeley Laboratory, University of California, 1974, pp. 197-260.
6. Satchler, G. R.; and Love, W. G.: Folding Model Potentials From Realistic Interactions for Heavy-Ion Scattering. Physics Rep., vol. 55, no. 3, 1979, pp. 183-254.

ORIGINAL PAGE IS
OF POOR QUALITY

7. Wilson, J. W.; and Townsend, L. W.: An Optical Model for Composite Nuclear Scattering. Canadian Journal of Physics, vol. 59, no. 11, 1981, pp. 1569-1576.
8. De Jager, C. W.; De Vries, H.; and De Vries, C.: Nuclear Charge- and Magnetization-Density-Distribution Parameters From Elastic Electron Scattering. At. Data & Nucl. Data Tables, vol. 14, no. 5/6, 1974, pp. 479-508.
9. Skrzypczak, E.: Cross-Sections for Inelastic ^4He and ^{12}C -Nucleus Collisions at 4.5 GeV/c/N Incident Momentum. Proceedings of the International Conference on Nuclear Physics, Volume 1, Abstracts, LBL-11118 (Contract No. W-7405-ENG-48), Lawrence Berkeley Laboratory, University of California, 1980, p. 575.

Table I
Fermi Momenta versus Mass Number (from reference 4)

Mass Number A	k_F , fm ⁻¹
6	0.856
12	1.120
24	1.191
40	1.272
59	1.318
89	1.287
119	1.318
181	1.343
208	1.343

Table II

Abrasion Cross Sections for $^{20}\text{Ne} + ^{12}\text{C} \rightarrow n + X$
 (incident kinetic energy is 2.1 GeV/nucleon).

Number of Abraded nucleons, n	Abrasion Cross Sections, mb			
	$r_c = 0.87 \text{ fm}$			$r_c = .806 \text{ fm}$
	$k_F = 1.36 \text{ fm}^{-1}$	$k_F = 1.23 \text{ fm}^{-1}$	$k_F = 0.7 \text{ fm}^{-1}$	$k_F = 0.7 \text{ fm}^{-1}$
1	248	241	241	252
2	134	131	131	136
3	96	93	93	96
4	76	74	74	77
5	64	63	63	65
6	57	56	56	57
7	52	50	50	52
8	48	47	47	48
9	45	44	44	46
10	43	42	42	44
11	42	41	41	42
12	40	39	39	40
13	37	37	36	36
14	33	33	32	31
15	26	26	25	24
16	18	18	16	16
17	10	10	9	8
18	4	4	4	3
19	1	1	1	0.8
20	0.1	0.1	0.1	0.1
σ_{abs}	1074	1051	1044	1074

Table III

Relative Probabilities for Formation of Projectile
Fragment A_F for Ne + C

A_F	Relative Probability			
	$r_c = 0.87 \text{ fm}$			$r_c = .806 \text{ fm}$
	$k_F = 1.36 \text{ fm}^{-1}$	$k_F = 1.23 \text{ fm}^{-1}$	$k_F = 0.7 \text{ fm}^{-1}$	$k_F = 0.7 \text{ fm}^{-1}$
19	.131	.130	.131	.133
18	.141	.140	.141	.143
17	.101	.100	.101	.102
16	.080	.080	.080	.081
15	.068	.068	.068	.068
14	.060	.060	.060	.060
13	.054	.054	.055	.055
12	.050	.050	.051	.051
11	.048	.048	.048	.048
10	.046	.046	.046	.046
9	.044	.044	.044	.044
8	.042	.042	.042	.042
7	.039	.040	.039	.038
6	.035	.035	.034	.033
5	.027	.028	.027	.025
4	.019	.019	.019	.016
3	.010	.011	.010	.009
2	.004	.004	.004	.003
1	.001	.001	.001	.0008
0	.0001	.0001	.0001	.0001

ORIGINAL PAGE IS
OF POOR QUALITY

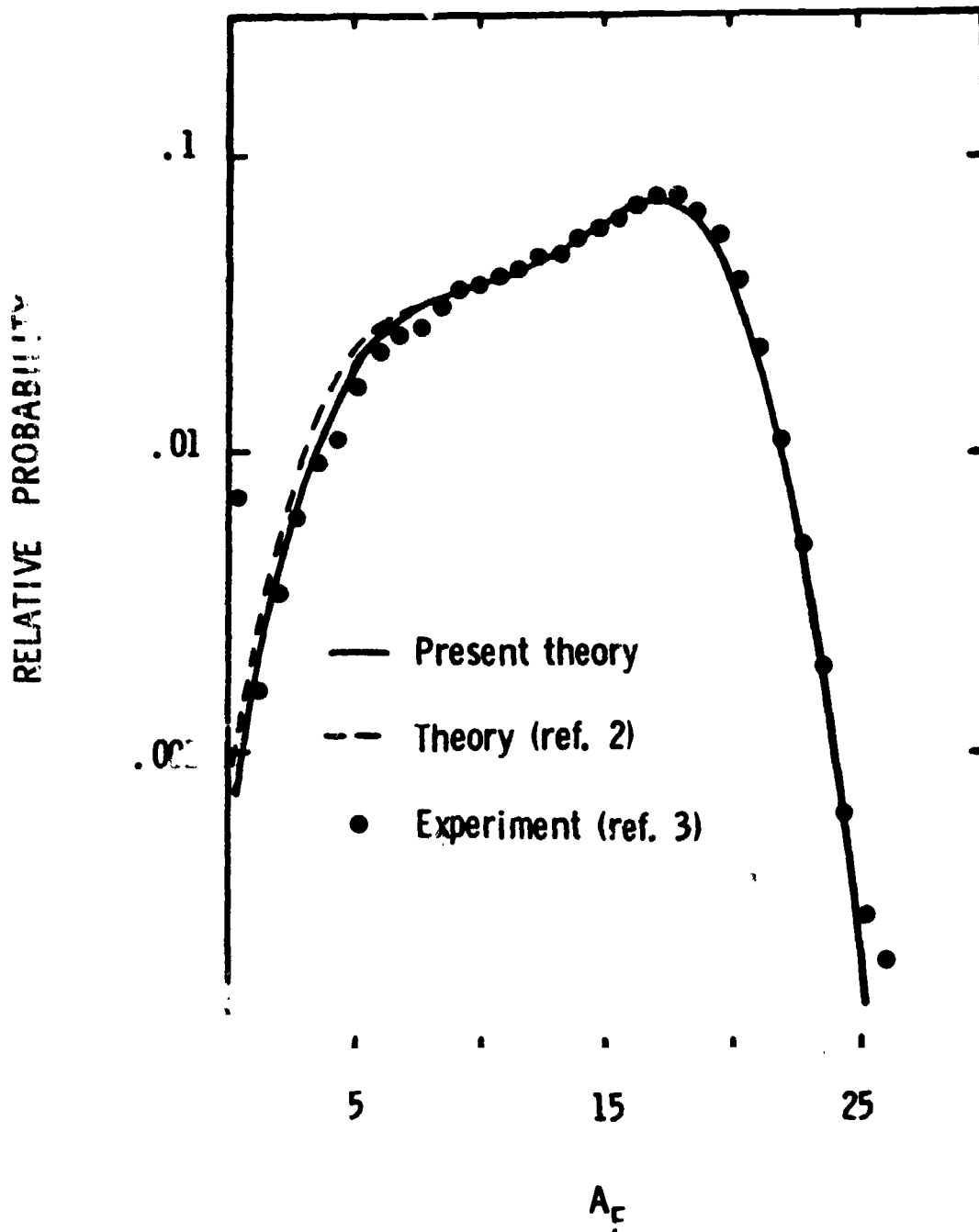


Figure 1. Abrasion results for neon projectiles colliding with carbon targets, as predicted by this work and the previous abrasion model (ref. 2), compared with experiment. Incident kinetic energy is 2.1 GeV/nucleon.

ORIGINAL PAGE IS
OF POOR QUALITY

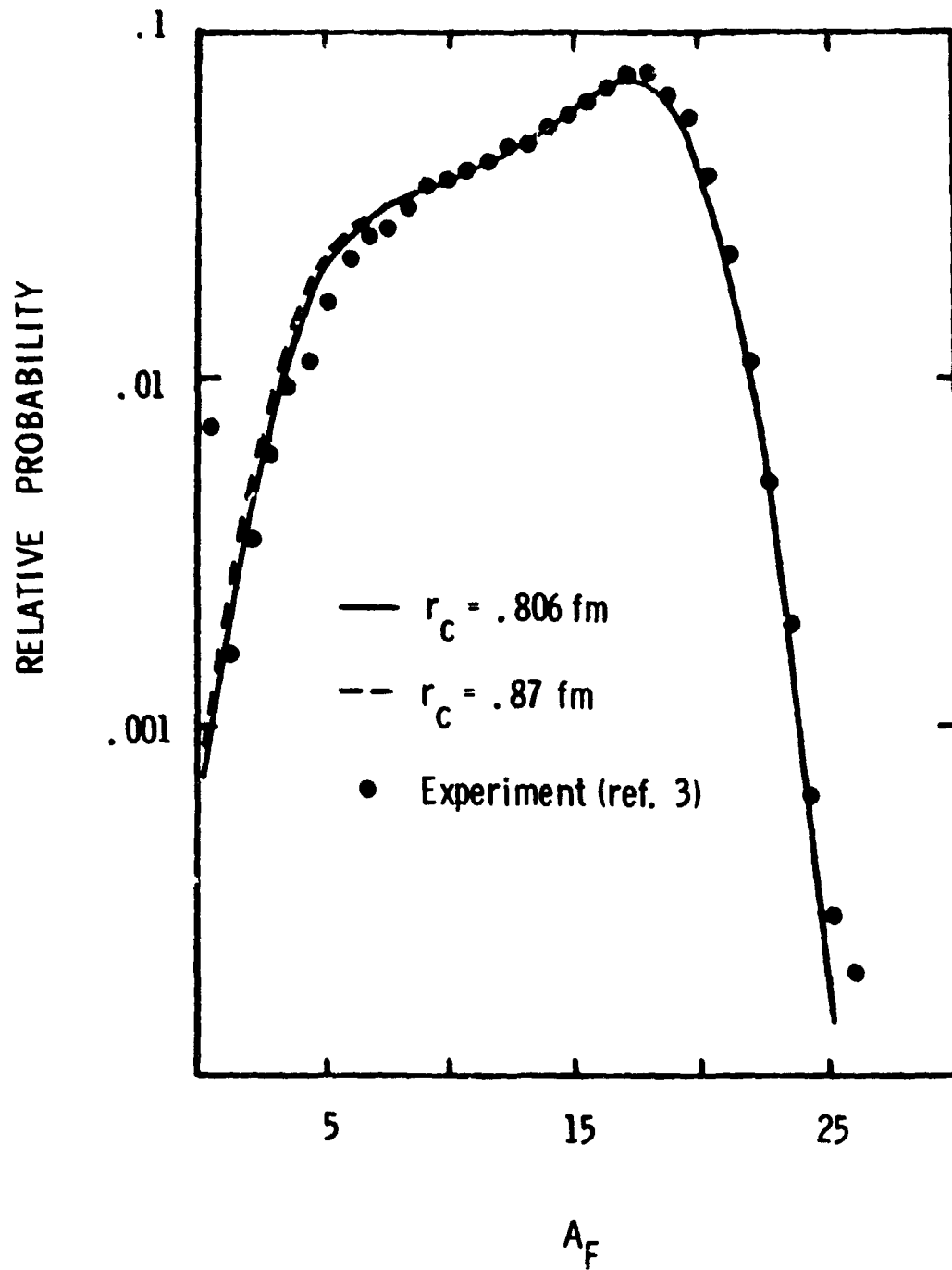


Figure 2. Abrasion results for neon projectiles colliding with carbon targets, as a function of nucleon rms charge radius, r_c , compared with experiment. Incident kinetic energy is 2.1 GeV/nucleon.

ORIGINAL PAGE IS
OF POOR QUALITY

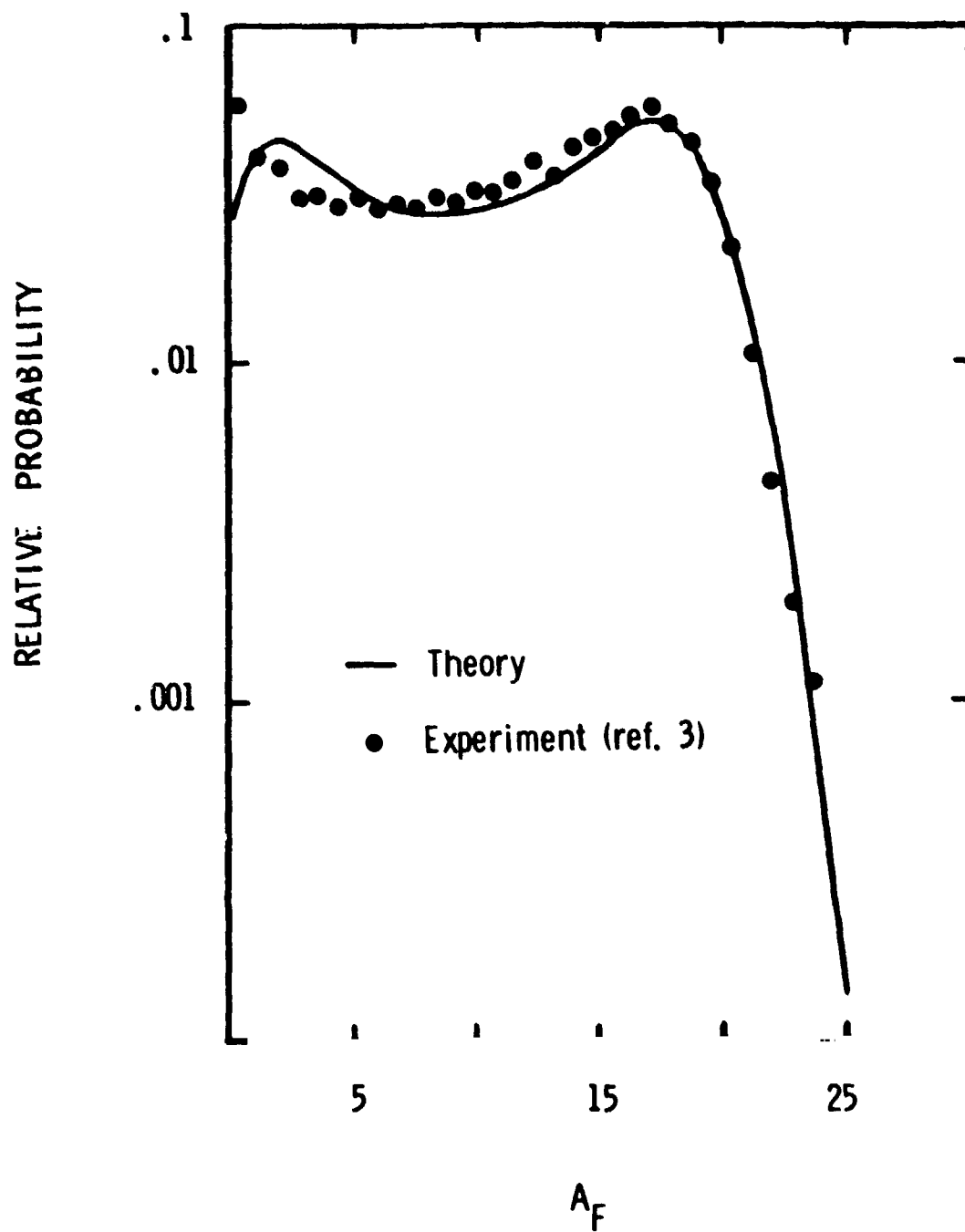


Figure 3. Abrasion results for neon projectiles colliding with molybdenum targets. Incident kinetic energy is 2.1 GeV/nucleon.